CellPress
PARTNER JOURNAL

Molecular Plant
Research Article

Dynamic and Antagonistic Allele-Specific Epigenetic Modifications Controlling the Expression of Imprinted Genes in Maize Endosperm

Xiaomei Dong[1,3], Mei Zhang[1,2,3], Jian Chen[1,3], Lizeng Peng[1], Nan Zhang[1], Xin Wang[1] and Jinsheng Lai[1,*]

[1]State Key Laboratory of Agrobiotechnology and National Maize Improvement Center, Department of Plant Genetics and Breeding, China Agricultural University, Beijing 100193, P.R. China

[2]Department of Biology, Stanford University, Stanford, CA 94305, USA

[3]These authors contributed equally to this article.

***Correspondence: Jinsheng Lai (jlai@cau.edu.cn)**

http://dx.doi.org/10.1016/j.molp.2016.10.007

ABSTRACT

Genomic imprinting is often associated with allele-specific epigenetic modifications. Although many reports suggested potential roles of DNA methylation and H3K27me3 in regulating genomic imprinting, the contributions of allele-specific active histone modifications to imprinting remain still unclear in plants. Here, we report the identification of 337 high-stringency allele-specific H3K4me3 and H3K36me3 peaks in maize endosperm. Paternally preferred H3K4me3 and H3K36me3 peaks mostly co-localized with paternally expressed genes (PEGs), while endosperm-specific maternally expressed genes (endo-MEGs) were associated with maternally preferred H3K4me3 and H3K36me3 peaks. A unique signature for PEGs was observed, where the active H3K4me4 and H3K36me3 as well as repressive H3K27me3 appeared together. At the gene body of con-PEGs (constitutively expressed PEG), H3K27me3 and H3K36me3 were specifically deposited on hypomethylated maternal alleles and hypermethylated paternal alleles, respectively. Around the transcription start sites of endo-MEGs, DNA methylation and H3K4me3 specifically marked paternal and maternal alleles, respectively. In addition, 35 maternally expressed non-coding RNAs exhibited the same allele-specific epigenetic features as endo-MEGs, indicating similar mechanisms for the regulation of imprinted genes and non-coding RNAs. Taken together, our results uncover the complex patterns of mutually exclusive epigenetic modifications deposited at different alleles of imprinted genes that are required for genomic imprinting in maize endosperm.

Key words: genomic imprinting, H3K4me3, H3K36me3, endosperm, maize

Dong X., Zhang M., Chen J., Peng L., Zhang N., Wang X., and Lai J. (2017). Dynamic and Antagonistic Allele-Specific Epigenetic Modifications Controlling the Expression of Imprinted Genes in Maize Endosperm. Mol. Plant. **10**, 442–455.

INTRODUCTION

Genomic imprinting, a classic epigenetic phenomenon identified first in maize (Kermicle and Alleman, 1990), arises from allele-specific epigenetic modifications that are generally believed to be established during gametogenesis (Huh et al., 2008; Raissig et al., 2011; Kawashima and Berger, 2014). In flowering plants, genomic imprinting occurs primarily in the endosperm, which provides an energy source for embryos and germinating seeds. So far, several hundred imprinted genes have already been identified in a number of species such as *Arabidopsis*, rice, maize, sorghum, and caster bean (Gehring et al., 2011; Hsieh et al., 2011; Luo et al., 2011; Waters et al., 2011; Wolff et al., 2011; Zhang et al., 2011, 2016; Xin et al., 2013). One of the major questions on imprinting in plant endosperm is how the allele-specific epigenetic modifications are established to determine the parent-of-origin-dependent expression of imprinted genes.

DNA methylation is an important epigenetic modification involved in regulating gene expression. Several studies have shown that

Published by the Molecular Plant Shanghai Editorial Office in association with Cell Press, an imprint of Elsevier Inc., on behalf of CSPB and IPPE, SIBS, CAS.

DNA methylation plays an important role in the allele-specific expression of imprinted genes. A number of maternally expressed imprinted genes (MEGs) and paternally expressed imprinted genes (PEGs) are shown to be regulated by the DNA demethylation glycosylase DEMETER and/or the DNA methyltransferase MET1 in *Arabidopsis* (Kinoshita et al., 2004; Jullien et al., 2006; Tiwari et al., 2008; Hsieh et al., 2011; Wolff et al., 2011). In addition, many imprinted genes are associated with differentially methylated regions (DMRs) where the maternal alleles are hypomethylated and the paternal alleles are hypermethylated (Lund et al., 1995a, 1995b; Gutierrez-Marcos et al., 2004, 2006; Haun et al., 2007; Jahnke and Scholten, 2009; Du et al., 2014). The genome-wide high-resolution allele-specific DNA methylation maps and their association with the allele-specific expression of MEGs and PEGs have been established recently in *Arabidopsis*, rice, and maize endosperm (Zhang et al., 2011; Ibarra et al., 2012; Rodrigues et al., 2013; Zhang et al., 2014a).

Histone modifications represent another layer of epigenetic modifications. Genome-wide analyses have demonstrated that several types of histone modifications are associated with the expression or repression of genes in many organisms (Li et al., 2008; Wang et al., 2009; Zhang et al., 2009). For instance, H3K4me3, H3K36me3, and H3K9Ac are typically associated with transcriptional activation, while H3K27me3 and H3K9me2 are associated with transcriptional repression in general. Repressive histone modification H3K27me3 mediated by POLYCOMB REPRESSIVE COMPLEX 2 (PRC2) was shown to be involved in the monoallelic expression of some imprinted genes in plants. For example, the expression of the *PHERES1* (*PHE1*), a PEG in *Arabidopsis*, required PRC2 targeting and silencing of its maternal allele (Kohler et al., 2005). The imprinting of many other MEGs and PEGs was also reported to be subjected to regulation of the repressive PRC2 complex through analysis of the transcriptome of *fie* or *fis2* endosperm in *Arabidopsis* (Hsieh et al., 2011; Wolff et al., 2011). In rice, maternally preferred H3K27me3 in the gene body is required for the paternal expression of *OsYUCCA1* (Du et al., 2014). Genome-wide allele-specific maps of H3K27me3 in maize endosperm indicated that maternally preferred H3K27me3 peaks tend to locate around PEGs to silence the expression of maternal alleles (Zhang et al., 2014a). In contrast to the many reports about the requirement of repressive histone modification on imprinting regulation, there is very limited genome-wide information about the contribution of active histone modifications to the allele-specific expression of imprinted genes in plants, although the maternally enriched expression of three MEGs (*Mez1*, *Fie1*, and *Nrp1*) were reported to require H3K4me2, H3, and H4 acetylation (Haun and Springer, 2008).

Here, we reported the allele-specific profiles of H3K4me3 and H3K36me3 modifications on a genome-wide scale in the endosperm of maize at 12 days after pollination (DAP). More than 300 allelic-specific H3K4me3 and H3K36me3 peaks localized to discrete genic and intergenic regions were found to associate with both imprinted protein-coding genes and imprinted non-coding RNAs. Integration of the allele-specific active histone modifications (H3K4me3 and H3K36me3) with allele-specific DNA methylation and repressive modification (H3K27me3) provides a unique opportunity to understand the regulation of genomic imprinting in maize.

RESULTS

Identification of Parent-of-Origin-Dependent H3K4me3 and H3K36me3 Peaks in Maize Endosperm

To investigate how active histone modifications contribute to gene imprinting on a genome-wide scale, we performed RNA-seq and ChIP-seq for 12 DAP maize endosperm from reciprocal crosses of B73 and Mo17 inbred (B73 × Mo17 and Mo17 × B73) with histone H3 lysine 4 trimethylation (H3K4me3) and lysine 36 trimethylation (H3K36me3) antibodies (Supplemental Table 1). Consistent with previous work on H3K4me3 and H3K36me3 profiles at genes in maize shoot and root (Wang et al., 2009), H3K4me3 modifications were generally restricted to the transcription start sites (TSS), and H3K36me3 modifications were accumulated to high levels in gene bodies (Figure 1A and 1B). Both H3K4me3 and H3K36me3 showed positive correlation with transcriptional levels in maize endosperm (Figure 1A and 1B).

A total of 38,139 H3K4me3 peaks and 21,833 H3K36me3 peaks were identified in B73 × Mo17 (BM) and Mo17 × B73 (MB) endosperm samples by using MACS software (Figure 1C) (Feng et al., 2012). Among the peaks identified, 23,493 H3K4me3 and 15,221 H3K36me3 peaks covering at least two SNPs and having at least 10 reads on both B73 and Mo17 alleles were used for identifying allele-specific peaks (Figure 1C). As a result, 1,393 H3K4me3 peaks and 980 H3K36me3 peaks showed significant allelic bias (χ^2 test; $p < 0.05$) in both BM and MB endosperm. Using a more stringent criteria (>85% of reads from the maternal allele or >60% of the reads from the paternal allele in both BM and MB endosperm), a total of 337 high-stringency allele-specific H3K4me3 and H3K36me3 peaks were identified, including 174 maternally preferred H3K4me3 (mH3K4me3) peaks, 30 paternally preferred H3K4me3 (pH3K4me3) peaks, 75 maternally preferred H3K36me3 (mH3K36me3) peaks, and 58 paternally preferred H3K36me3 (pH3K36me3) peaks (Figure 1C). These results are quite different from the allele-specific pattern of H3K27me3 where only maternally preferred peaks were identified (Zhang et al., 2014a). To validate our results above, four randomly selected candidate H3K4me3 and H3K36me3 peaks were tested by quantitative real-time PCR. All four selected loci exhibited significant enrichment for antibody compared with the control (Supplemental Figure 1). Sanger sequencing of RT–PCR amplicons from 12 DAP BM and MB endosperm for mH3K4me3, mH3K36me3, pH3K4me3, and pH3K36me3 peaks proved the accuracy of allele-specific peaks (Supplemental Figure 2). The preferred location of the pH3K4me3 and pH3K36me3 peaks was in genic regions (80%–90%), while only about 60% of mH3K4me3 and mH3K36me3 peaks were located in genic regions (Figure 1D), indicating that some mH3K4me3 and mH3K36me3 peaks (~40%) may present in non-coding regions, nearly half of which were located in non-transposable element intergenic regions.

Co-localization of the Allele-Specific H3K4me3 and H3K36me3 Peaks

Since H3K4me3 and H3K36me3 are both tightly associated with active transcription, we investigated the co-localization of the parent-of-origin-dependent H3K4me3 and H3K36me3

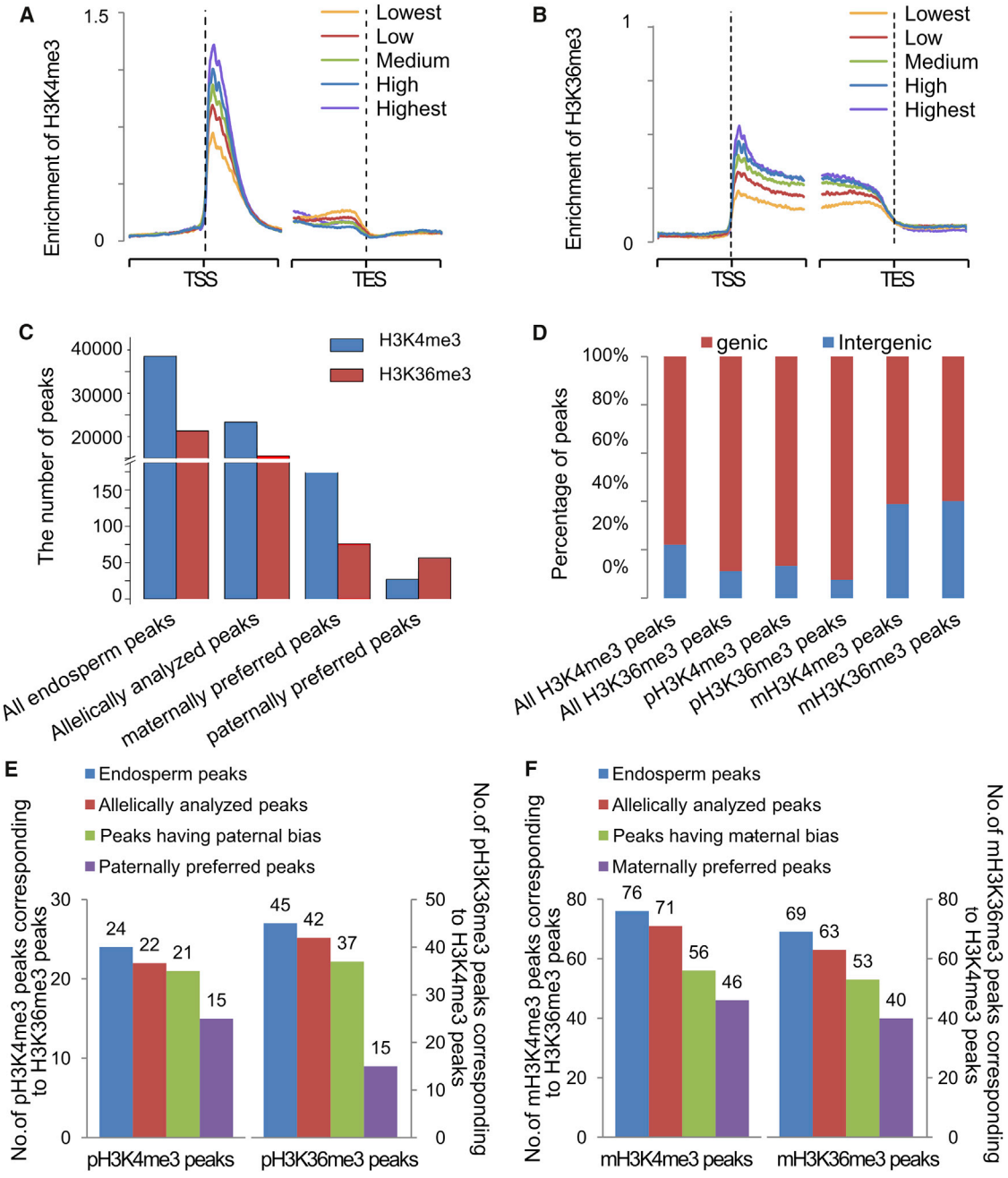

Figure 1. The Characteristics of H3K4me3 and H3K36me3 Peaks in Maize Endosperm.

(A and B) The enrichment profiles of H3K4me3 and H3K36me3 in genes with different expression levels. The expressed genes (FPKM $\geq$1) were divided into five clusters based on their expression levels.

(C) The number of all H3K4me3 and H3K36me3 peaks, allelically analyzable H3K4me3 and H3K36me3 peaks, high-stringency maternally preferred H3K4me3 and H3K36me3 peaks, and paternally preferred H3K4me3 and H3K36me3 peaks are shown.

(D) The proportion of allelic-specific H3K4me3 and H3K36me3 peaks in the genic or intergenic region of the maize genome. The genic region includes the gene body and the region 2 kb up and down.

(E) The number of high-stringency pH3K4me3 peaks overlapping with all H3K36me3 peaks, allelically analyzable H3K36me3 peaks, H3K36me3 peaks showing paternal bias, and high-stringency pH3K36me3 peaks (left). The number of high-stringency pH3K36me3 peaks overlapping with all H3K4me3 peaks, allelically analyzable H3K4me3 peaks, H3K4me3 peaks showing paternal bias, and high-stringency pH3K4me3 peaks (right). The numbers above the bars indicate the number of high-stringency pH3K36me3 (left), high-stringency pH3K36me3 (right) overlapping with corresponding peaks.

(F) The number of high-stringency mH3K4me3 peaks overlapping with all H3K36me3 peaks, allelically analyzable H3K36me3 peaks, H3K36me3 peaks showing maternal bias, and high-stringency mH3K36me3 peaks (left). The number of high-stringency mH3K36me3 peaks overlapping with all H3K4me3 peaks, allelically analyzable H3K4me3 peaks, H3K4me3 peaks showing maternal bias, and high-stringency mH3K4me3 peaks (right). The numbers above the bars indicate the number of high-stringency mH3K36me3 (left), high-stringency mH3K36me3 (right) overlapping with corresponding peaks.

peaks. For 30 pH3K4me3 peaks, 24 (80%) had corresponding H3K36me3 peaks (Figure 1E). Of 22 pH3K4me3 peaks overlapped with allelically analyzed H3K36me3 peaks (having enough reads for allelic enrichment analysis), 21 (95.5%) overlapped with significantly paternal bias H3K36me3 peaks, and 15 (71.4%) overlapped with high-stringency pH3K36me3 peaks (Figure 1E). Similarly, 88.1% (37/42) of pH3K36me3 overlapped with significantly paternal bias H3K4me3 peaks (Figure 1E). These results indicate that pH3K4me3 and pH3K36me3 peaks mostly co-localize to each other.

We also analyzed the co-localization of mH3K4me3 and mH3K36me3 peaks. For mH3K36me3 peaks, 84.1% (53/63) overlapped with significantly maternal bias H3K4me3 peaks (Figure 1F). Only 43.7% (76) of mH3K4me3 peaks had corresponding H3K36me3 peaks (Figure 1F), although 78.9% (56/71) overlapped with significantly maternal bias H3K36me3 peaks (Figure 1F). To clarify why about half of the mH3K4me3 peaks cannot overlap with H3K36me3 peaks, we checked the genome distribution of mH3K4me3 peaks without corresponding H3K36me3 peaks, and found that 26% of which were located in the intron of active genes (Supplemental Figure 3A). We speculated that the intronic H3K36me3 peaks were almost indistinguishable from the H3K36me3 peaks deposited on the whole body of the active genes, just as the H3K4me3 and H3K36me3 peaks located on GRMZM2G471115 (Supplemental Figure 3C). Moreover, we found that the remaining 74% of mH3K4me3 peaks without corresponding H3K36me3 peaks tended to mark protein-coding genes with low expression levels or intergenic regions with low coverage (Supplemental Figure 3B), so that the enrichment levels of corresponding H3K36me3 were too low to be identified as peaks. Therefore, most mH3K4me3 peaks would have corresponding mH3K36me3 peaks although some cannot be identified due to the limitations of the method and the sequencing depth. Overall, similar to the pH3K4me3 and pH3K36me3 peaks, the mH3K4me3 and mH3K36me3 peaks also mostly co-localize to each other.

Relationship between Imprinted Genes and the Allele-Specific H3K4me3 and H3K36me3 Peaks

Deep RNA-seq using samples isolated from 12 DAP hybrid endosperm tissues from the reciprocal crosses between B73 and Mo17 were performed to identify imprinted genes. A total of 54 MEGs and 90 PEGs were identified using previously reported highly stringent criteria (Zhang et al., 2011, 2014a), where the expression level of active alleles must be at least five times that of silenced alleles (Supplemental Table 3). The majority (81.0%) of imprinted genes in this study were also identified in previous works in which imprinted genes were identified using samples of 10 and 14 DAP endosperm (Waters et al., 2011; Zhang et al., 2011). Meanwhile, 64.1% of imprinted genes in the two earlier publications were identified in this study. The majority of imprinted genes identified in the two earlier studies but not included this time were not highly expressed (fragments per kilobase of transcript per million mapped reads [FPKM] <1) in 12 DAP endosperm or did not reach our stringency criteria, although showing allelic expression. Then, imprinted genes were divided into subgroups based on their pattern of expressional tissue specificity (Supplemental Figure 4). Twenty-eight constitutive MEGs (con-MEGs), 24 endosperm-specific MEGs (endo-MEGs), 70 constitutive PEGs (con-PEGs), and 20 endosperm-specific PEGs (endo-PEGs) were obtained.

To investigate the roles of H3K4me3 and H3K36me3 in the regulation of genomic imprinting, we analyzed the allelic status of H3K4me3 and H3K36me3 peaks located around imprinted genes. Like all actively transcribed genes (FPKM $\geq$1) in endosperm (Figure 2A), most of the endo-MEGs, con-PEGs, and endo-PEGs (79%–100%) possessed H3K4me3 and H3K36me3 peaks, whereas 80% of con-MEGs possessed H3K4me3 peaks and only 3 (13.3%) con-MEGs overlapped with endosperm H3K36me3 peaks (Figure 2A). The possible reasons for the poor correlation between con-MEGs and H3K36me3 modification are discussed later. As observed, most of the H3K4me3 and H3K36me3 peaks at endo-MEGs were preferentially enriched on maternal alleles (Figure 2B). For 21 and 19 endo-MEGs overlapped with allelically analyzed H3K4me3 and H3K36me3 peaks, 85% and 84.2% were associated with H3K4me3 and H3K36me3 peaks with significant maternal bias, and 50% and 73.7% were significantly associated with high-stringency mH3K4me3 and mH3K36me3 peaks compared with non-imprinted genes (Fisher test; both $p < 2.2e-16$), respectively (Figure 2C). By contrast, the H3K4me3 and H3K36me3 peaks at both con-PEGs and endo-PEGs displayed significantly preferred enrichment on paternal alleles (Figure 2B). For 62 and 67 con-PEGs overlapped with allelically analyzed H3K4me3 and H3K36me3 peaks, 71.0% and 95.5% were associated with H3K4me3 and H3K36me3 peaks with significant paternal bias, and 22.3% and 43.3% were significantly associated with high-stringency pH3K4me3 and pH3K36me3 peaks (Fisher test; both $p < 2.2e-16$), respectively (Figure 2C). For 17 and 16 endo-PEGs overlapped with allelically analyzed H3K4me3 and H3K36me3 peaks, 82.3% and 87.5% were associated with H3K4me3 and H3K36me3 peaks with significant paternal bias, and 35.3% and 68.8% were significantly associated with high-stringency pH3K4me3 and pH3K36me3 peaks (Fisher test; both $p < 2.2e-16$), respectively (Figure 2C). Hence, the allele-specific transcription of endo-MEGs, con-PEGs, and endo-PEGs were significantly associated with allele-preferred deposition of H3K4me3 and H3K36me3, which are two active histone modifications correlated with transcription initiation and elongation (Barski et al., 2007; Guenther et al., 2007).

The profiles of epigenetic modifications at GRMZM2G170099 (endo-MEG), which encodes a PHD finger family protein, are displayed in Supplemental Figure 5A. Both H3K4me3 and H3K36me3 modifications at GRMZM2G170099 prefer to enrich on maternal alleles. The integrated view of GRMZM2G110306 (con-PEG) and GRMZM2G127160 (*ZmTar*, endo-PEG) are shown in Supplemental Figure 5B and 5C, encoding an AT-rich interactive domain-containing protein and a tryptophan-aminotransferase-related protein, respectively. As shown in Supplemental Figure 5B and 5C, almost all SNPs within the H3K4me3 and H3K36me3 peaks located at two PEGs exhibited significantly paternal bias.

PEGs Are Characterized by Possessing H3K4me3, H3K36me3, and H3K27me3 Modifications Altogether in Endosperm

Using the data of H3K27me3 we generated previously (Zhang et al., 2014a), we were able to investigate the involvement of

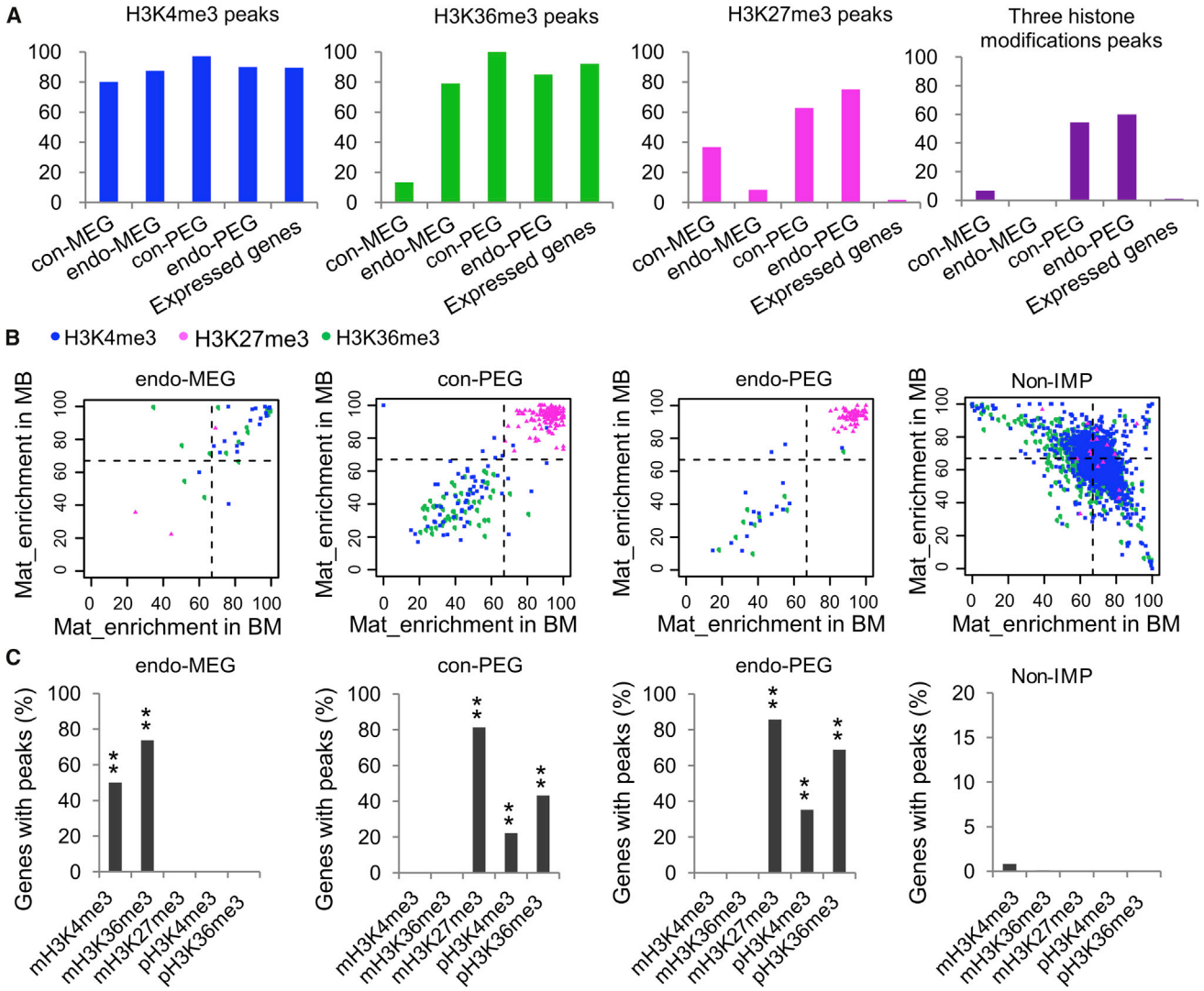

Figure 2. Relationship between H3K4me3, H3K36me3, and H3K27me3 Modifications and Subgroups of Imprinted Genes.

(A) The proportion of genes overlapping with all H3K4me3, H3K36me3, and H3K27me3 peaks identified in maize endosperm. con-MEGs, MEGs expressed in many tissues; endo-MEGs, MEGs expressed specifically in endosperm; con-PEGs, PEGs expressed in many tissues; endo-PEGs, PEGs expressed specifically in endosperm; expressed genes, all genes with FPKM $\geq$1 in endosperm.

(B) Allele-specific analysis of H3K4me3, H3K36me3, and H3K27me3 peaks at imprinted genes and non-imprinted genes. The x axis and y axis represent the proportion of maternal reads for the peaks that had at least two SNPs and had at least 10 allelic reads in both reciprocal hybrids. The blue, green, and pink points represent the allelic status of H3K4me3, H3K36me3, and H3K27me3 peaks at genes, respectively. Non-imprinted genes, genes not significantly deviating from a 2:1 ratio of maternal allele to paternal allele in both reciprocal hybrids.

(C) Association of imprinted genes and non-imprinted genes with allele-specific H3K4me3, H3K36me3, and H3K27me3 peaks. The x axis represents high-stringency maternally preferred H3K4me3 (mH3K4me3) peaks, maternally preferred H3K36me3 (mH3K36me3) peaks, maternally preferred H3K27me3 (mH3K27me3) peaks, paternally preferred H3K4me3 (pH3K4me3) peaks, and paternally preferred H3K36me3 (pH3K36me3) peaks. The proportions of imprinted genes and non-imprinted genes with those allele-specific peaks are shown on the y axis. Asterisks represents significant association of imprinted genes with allele-specific peaks (Fisher test; $p < 0.001$), compared with that of non-imprinted genes.

both the active (H3K4me3 and H3K36me3) and repressive (H3K27me3) histone modifications at imprinted genes in the same time. Interestingly, we found that 38 (54.3%) con-PEGs and 12 (60%) endo-PEGs had H3K4me3, H3K36me3, and H3K27me3 peaks, contrasting with 6.7% of con-MEGs, no endo-MEGs, and 1.7% of non-imprinted genes (Figure 2A). Because the enrichment of H3K27me3 modification was overall less than that of H3K36me3 and H3K4me3 (Supplemental Figure 6), the number of H3K27me3 peaks could be underestimated under the same strict criteria of calling peaks. When H3K27me3 peaks that existed only in BM or MB endosperm were included, 70 (78.9%) PEGs contained all three histone marks. To test if such a pattern of histone marks was specific for PEGs, we scanned the regions with all three H3K4me3, H3K36me3, and H3K27me3 peaks in maize endosperm for the entire genome. The H3K27me3 peaks rarely overlapped with the H3K4me3 and H3K36me3 peaks in maize endosperm (Supplemental Figure 7A), in agreement with

previous reports that active H3K4me3 and H3K36me3 are mutually exclusive with H3K27me3 modifications (Pasini et al., 2008; Schmitges et al., 2011; Brien et al., 2012). Nevertheless, we identified 240 loci (locating at 229 genes) with all three histone modifications in the whole genome. Among the 229 genes, 104 (45.4%) genes cannot be allelically analyzed due to the lack of exonic SNPs between B73 and Mo17 inbred or not enough RNA-seq reads on SNPs (Supplemental Figure 7B). For the remaining 125 genes, 84 (70%) genes exhibited a preferential paternal expression, including 50 high stringent PEGs (Supplemental Figure 7B). For 81 genes without exonic SNPs between B73 and Mo17 inbreds, we further investigated their allelic status in four additional reciprocal hybrids generated by crossing inbred lines Ki11 and Oh43 with both B73 and Mo17 (Waters et al., 2013). The results showed that among 46 allelically analyzed genes, 30 (65.2%) genes exhibited preferential paternal expression in any one of reciprocal hybrids, where the proportion may be underestimated due to the existence of allelic imprinting (Supplemental Figure 7C). Our results indicate that possessing both active (H3K4me3, H3K36me3) and repressive (H3K27me3) histone modifications is a distinct feature for PEGs, which would be helpful to identify PEGs from those genes without SNPs in exonic regions.

We next characterized the allelic status of three histone modifications at PEGs. Compared with H3K4me3 and H3K36me3, which were preferentially accumulated on active paternal alleles, H3K27me3 preferentially accumulated on silent maternal alleles for more than 80% of con-PEGs, and endo-PEGs are associated with mH3K27me3 peaks (Zhang et al., 2014a) (Figure 2B and 2C). Therefore, the opposite patterns of H3K4me3, H3K36me3, and H3K27me3 peaks occur together in con-PEGs and endo-PEGs, with H3K4me3 and H3K36me3 deposited on active paternal alleles and H3K27me3 deposited on repressive maternal alleles.

Integrated Profiles of Allele-Specific DNA Methylation and Histone Modifications at Imprinted Genes

Our previous work indicated that endo-MEGs and con-PEGs are associated with DMRs where the maternal alleles are hypomethylated and the paternal alleles are hypermethylated (pDMRs) (Zhang et al., 2014a). Here, we investigated the relationship of parent-of-origin-dependent H3K4me3, H3K36me3, H3K27me3 peaks and allele-specific DNA methylation at imprinted genes. For endo-MEGs, pDMRs (in both CG and CHG context) overlapping with mH3K4me3 peaks were located around TSS (Figure 3A and Supplemental Figure 8A), indicating that H3K4me3 is specifically deposited on the hypomethylated maternal alleles. For example, the CG_pDMR is located on the 5′ end of GRMZM2G170099, corresponding well with mH3K4me3 peaks (Supplemental Figure 5A). Furthermore, the DNA methylation levels (in both CG and CHG context) on the maternal alleles were significantly lower than those on paternal alleles in the region of mH3K4me3 peaks, different from the DNA methylation levels in the region of all H3K4me3 peaks exhibiting hypomethylation on both alleles (Figure 3C and 3D and Supplemental Figure 8C and 8D). About 78.7%/53.2% of mH3K4me3 peaks were significantly associated with CG_pDMRs/CHG_pDMRs (Fisher test; p (CG) <2.2e−16, p (CHG) <2.2e−16), while the proportion of that for all H3K4me3 peaks reduced to 8.4%/0.94% (Figure 3E and Supplemental Figure 8E). The results suggest that pDMRs and mH3K4me3 peaks can occur together around TSS for the regulation of allele-specific expression of imprinted genes.

For con-PEGs, CG_pDMRs (CHG_pDMRs preferentially locating on the upstream of con-PEGs) overlapping with mH3K27me3 and pH3K36me3 peaks were located throughout the gene body (Figure 3B and Supplemental Figure 8B), indicating that H3K27me3 specifically enriched on the hypomethylated maternal alleles while H3K36me3 preferentially enriched on hypermethylated paternal alleles. The epigenetic profile of GRMZM2G110306 is just an example (Supplemental Figure 5B). Furthermore, DNA methylation levels on maternal alleles were significantly lower than those on paternal alleles in the regions of pH3K36me3 peaks (Figure 3G). But there were no significantly differential methylation levels between parental alleles in the region of all H3K36me3 peaks (Figure 3F). About 57.1% of pH3K36me3 peaks were significantly associated with CG_pDMRs (Fisher test; p (CG) = 6.68e−11), while the corresponding proportion reduced to 6.2% for all H3K36me3 peaks (Figure 3H). Thus, pDMRs, mH3K27me3, and pH3K36me3 peaks occur together at the gene body of con-PEGs, which indicate complex imprinting regulation of con-PEGs involving DNA methylation and active and repressive histone modifications.

Imprinted Long Non-coding RNAs Are Highly Associated with Parent-of-Origin-Dependent Epigenetic Modifications

To investigate the allele-specific epigenetic modifications on imprinted non-coding RNAs, we identified 35 maternally specific expressed non-coding RNAs (MNCs) and two paternally specific expressed non-coding RNAs (PNCs) (Supplemental Table 4) in 12 DAP maize endosperm by assembling long non-coding RNAs and analyzing their allelic bias (see Methods). Due to the limited number of PNCs, we only discuss MNCs here. These MNCs tended to specifically express in endosperm (Supplemental Figure 9), in agreement with the results from reports that lncRNAs showed strong tissue-specific expression patterns (Cabili et al., 2011; Li et al., 2014; Zhang et al., 2014b). Twenty (57%) of the 35 MNCs are located in intergenic regions, the others are transcribed from the promoter or intronic region of 11 PEGs and four non-imprinted genes. In addition, we employed strand-specific RNA-seq data of 14 DAP BM endosperm to determine the potential transcription directions of the MNCs by aligning ssRNA-seq reads to MNCs. As a result, the transcriptional directions of 32 MNCs were determined. Among them, seven were antisense MNCs, including an MNC from the intronic region of GRMZM2G475503 previously verified by RT–PCR (Zhang et al., 2011). An antisense MNC located in the promoter of *ZmYuc1* (endo-PEG) was identified (Bernardi et al., 2012).

To explore whether epigenetic marks correlate with monoallelic expression of imprinted non-coding transcripts, we further investigated the allelic state of H3K4me3 and H3K36me3 peaks around MNCs. We found that 68.6% of MNCs overlapped with H3K4me3 and H3K36me3 peaks (Figure 4A). Of the H3K4me3

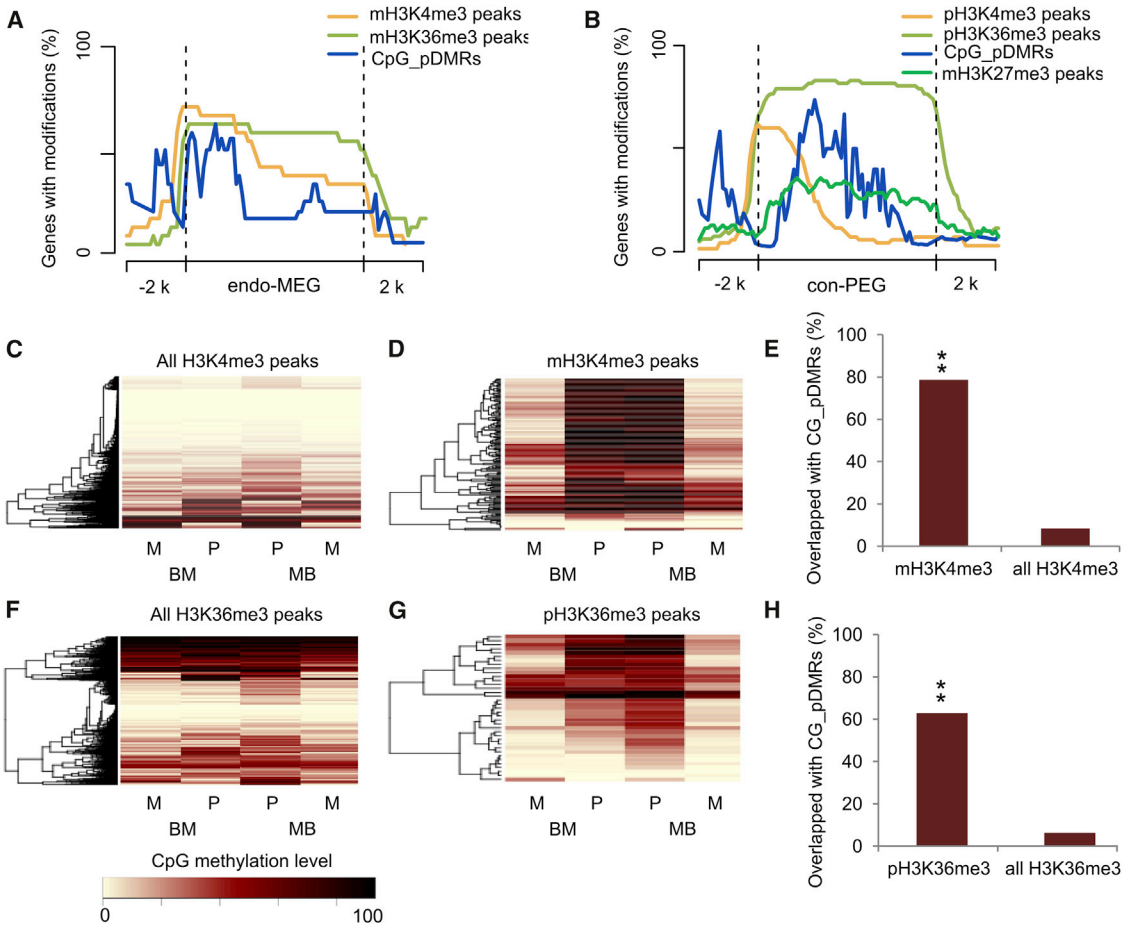

Figure 3. The Integrative Profiles of DNA Methylation and Histone Modifications.

(A and B) The distribution of CG_pDMRs, allele-specific H3K4me3, H3K36me3, and H3K27me3 peaks located at endo-MEGs, con-PEGs, and region 2 kb up- and downstream.

(C, D, F, and G) Heatmaps of CG methylation levels between alleles of B73 and Mo17 reciprocal crosses at all endosperm H3K4me3 peaks, maternally preferred H3K4me3 (mH3K4me3) peaks, all endosperm H3K36me3 peaks, and paternally preferred H3K36me3 (pH3K36me3) peaks. Only the region of peaks with at least one C site and at least 10 reads are shown. M, maternal allele; P, paternal allele; BM, B73 × Mo17; MB, Mo17 × B73.

(E and H) Association of all H3K4me3 peaks, maternally preferred H3K4me3 (mH3K4me3) peaks, all H3K36me3 peaks, and paternally preferred H3K36me3 (pH3K36me3) peaks with CG_pDMRs. The proportions of all H3K4me3 peaks and mH3K4me3 peaks with CG_pDMRs are shown on the y axis **(E)**. Asterisks represents significant association of mH3K4me3 peaks with CG_pDMRs (Fisher test; $p < 0.001$), compared with that of all H3K4me3 peaks. The proportions of all H3K36me3 peaks and mH3K36me3 peaks with CG_pDMRs are shown on the y axis **(H)**. Asterisks represents significant association of mH3K36me3 peaks with CG_pDMRs (Fisher test; $p < 0.001$), compared with that of all H3K36me3 peaks.

and H3K36me3 peaks overlapping with MNCs, 82.6% and 70.8% displayed maternally preferred enrichment, respectively (Figure 4A). Moreover, we also found 76.9% of MNCs overlapped with CG_pDMRs, located around TSS of MNCs (Figure 4B). Figure 4C showed the allelic state of H3K4me3 and H3K36me3 modifications on GRMZM2G406553 (PEG) and its antisense MNC. The CG_pDMRs were located in the gene body of GRMZM2G406553 but corresponding to the TSS of MNCs. The SNPs within the H3K4me3 and H3K36me3 peaks of MNC exhibited significantly maternal bias, while the H3K36me3 modification located in the gene body of GRMZM2G406553 was significantly enriched on the paternal allele.

There should be more imprinted long non-coding RNAs in endosperm. More than 90% of pH3K4me3 and pH3K36me3 peaks were associated with PEGs. Nevertheless, only 22% of mH3K4me3 peaks and 44% of mH3K36me3 peaks were associated with maternally expressed transcripts (endo-MEGs and MNCs) (Figure 4D and 4E). Excluding the mH3K4me3 and mH3K36me3 peaks overlapping with non-expressed or non-analyzed genes, the remaining 81 mH3K4me3 peaks and 20 mH3K36me3 peaks located in the intergenic region or intronic region presumably mark maternally expressed non-coding transcripts. But due to the low expression levels or method of identification, we did not obtain their corresponding transcripts in these regions. Here, we tried to investigate the allelic status of RNA-seq reads mapped in the region of these mH3K4me3 and mH3K36me3 peaks. Although only 18 mH3K4me3 peaks and eight mH3K36me3 peaks had at least 10 reads that could be assigned to a particular allele in each direction of the reciprocal crosses, all of them showed maternal specifically expression. So the mH3K4me3 peaks and mH3K36me3 in the

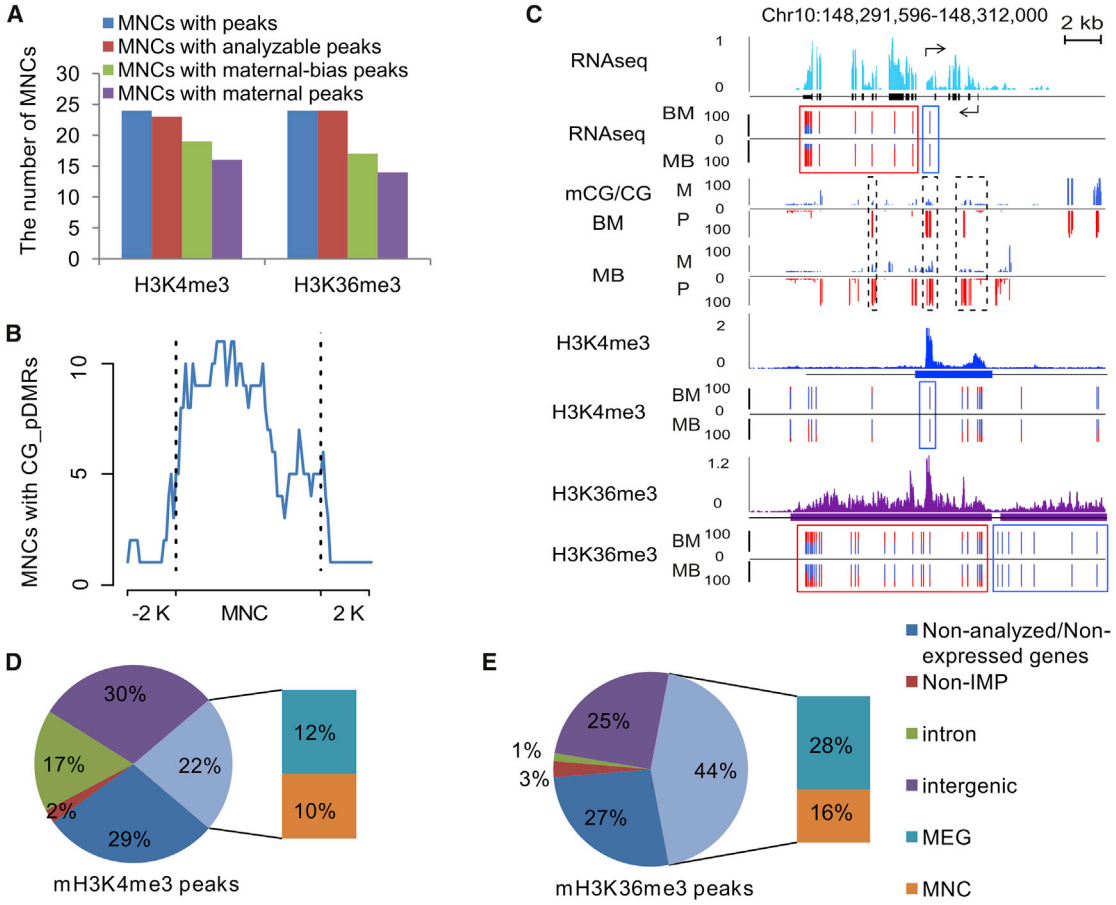

Figure 4. Relationship between MNCs and Parent-of-Origin DNA Methylation, H3K4me3, and H3K36me3 Peaks.

(A) The number of MNCs overlapping with all H3K4me3 peaks, allelically analyzable H3K4me3 peaks, H3K4me3 peaks showing maternal bias, and high-stringency mH3K4me3 peaks (left). The number of MNCs overlapping with all H3K36me3 peaks, allelically analyzable H3K36me3 peaks, H3K36me3 peaks showing maternal bias, and high-stringency mH3K36me3 peaks (right).

(B) The distribution of pDMRs located in MNCs and ±2 kb regions.

(C) Integrated views of H3K4me3, H3K36me3, H3K27me3, and DNA methylation at an MNC located in a PEG intron. The expression level of transcribed regions is shown in light blue for BM. The normalized levels of enrichment of H3K4me3 and H3K36me3 are plotted in blue and purple, respectively. The percentages of allelic reads of RNA-seq, H3K4me3, and H3K36me3 ChIP-seq data for specific SNP sites are shown, with red lines for the paternal allele and blue lines for the maternal allele. The DNA methylation level for specific SNP sites are shown for both maternal and paternal alleles, with red lines for the paternal allele (P) and blue lines for the maternal allele (M). Black rectangles represent the exon. The blue, purple, and pink rectangles highlight the H3K4me3, H3K36me3, and H3K27me3 peaks at genes. The dotted rectangles highlight the pDMRs identified in this region.

(D and E) Genomic distribution of high-stringency maternally preferred H3K4me3 and H3K36me3 peaks. Non-IMP represent non-imprinted genes that do not show significant deviation from a 2:1 ratio of maternal allele to paternal allele in each reciprocal hybrid. χ^2 (2:1, $p > 0.05$).

intergenic region or intronic region should correlate with the allele preference expression of corresponding non-coding RNAs.

DISCUSSION

Spatial Distribution of Imprinted Genes in Endosperm Compartments

Here, we reported the genome-wide allele-specific active histone modifications (H3K4me3 and H3K36me3) in 12 DAP maize endosperm. Integrated information on the allele-specific pattern of DNA methylation and histone modifications (H3K4me3, H3K36me3, and H3K27me3) is helpful for us to further gain insight into the regulation mechanism of monoallelic expression of imprinted genes and imprinted non-coding transcripts.

In this study, we did not investigate correlation of allele-specific epigenetic modifications with con-MEGs, as the correlation based on the current data with con-MEGs may be biased. Based on the previously reported data of gene expressional profiling from different endosperm compartments (Zhan et al., 2015), we found that con-MEGs rarely expressed in starchy endosperm, including central starchy endosperm and the conducting zone, which account for most of the area in 12 DAP endosperm (Supplemental Figure 10A). On the other hand, endo-MEGs, con-PEGs, and endo-PEGs tend to spread out in all different endosperm compartments. In contrast to most (75%–85%) endo-MEGs, con-PEGs, and endo-PEGs expressing in all endosperm compartments (FPKM ≥1), there were only four (14.3%) con-MEGs expressing in all endosperm compartments (Supplemental Figure 10B). Hence, we speculate that the poor

correlation between con-MEGs with epigenetic modifications is probably due to a sampling issue, as con-MEGs expressed in more specific endosperm compartments, but were not expressed to a great extent in the current endosperm samples used (mostly the starch endosperm).

Possible Epigenetic Silencing and Activation Dynamics at Imprinted Genes

The switch of active and repressive epigenetic marks can lead to activation or repression of the expression of genes (He et al., 2013; Widiez et al., 2014). In *Arabidopsis*, the opposing profiles of H3K36me3 and H3K27me3 in the *FLC* (*FLOWERING LOCUS C*) during the vernalization process is a good example of the antagonistic roles of H3K36me3 and H3K27me3 in the cold-induced epigenetic switch (Yang et al., 2014). In this study, the active and silent alleles of imprinted genes were deposited with mutually exclusive epigenetic modifications, implying that the potential epigenetic switch occurs at imprinted genes. Hence, we analyzed the integrated information on DNA methylation, H3K4me3, H3K36me3, and H3K27me3 modifications at the imprinted genes in 14 DAP shoots of B73 inbred (Wang et al., 2009; Li et al., 2015) to gain a better understanding of the possible epigenetic silencing and activation dynamics.

Endo-MEGs possessed a low proportion (8.3%–12.5%) of H3K4me3, H3K36me3, and H3K27me3 peaks in shoots (Supplemental Figure 11). The methylation pattern of endo-MEGs in shoots showed hypermethylation at TSS and the gene body (Zhang et al., 2014a). In endosperm, endo-MEGs were significantly associated with pDMRs, mH3K4me3, and mH3K36me3 peaks, which indicated that the epigenetic profiles at the silenced paternal alleles of endo-MEGs in endosperm accorded well with those in shoots. As we proposed before, the monoallelic expression of endo-MEGs is likely due to the activation of maternal alleles (Zhang et al., 2014a). Correspondingly, the dynamics of the silence to active state at maternal alleles of endo-MEGs possibly involves DNA demethylation and adding H3K4me3 and H3K36me3 modifications. To explore the activation of endo-MEGs occurring before or after fertilization, we also looked at the expression situation of 139 *Arabidopsis* imprinted genes in *Arabidopsis* central cells and 165 rice imprinted genes in rice sperm cells, respectively (Gehring et al., 2011; Hsieh et al., 2011; Luo et al., 2011; Wu et al., 2011; Schmid et al., 2012; Anderson et al., 2013). Based on the pattern of tissue specificity of expression, 77 con-MEGs, 37 endo-MEGs, 13 con-PEGs, and 12 endo-PEGs were obtained in *Arabidopsis*, and 46 con-MEGs, 47 endo-MEGs, 62 con-PEGs, and 10 endo-PEGs were obtained in rice. The results showed that most *Arabidopsis* endo-MEGs (62.2%) expressed in central cells (Supplemental Table 5), and rice endo-MEGs (68.1%) rarely expressed in sperm cells (Supplemental Table 6). So we hypothesized that DNA demethylation in central cells of the female gametophyte induced by *DME*-like protein presumably leads to hypomethylation at TSS of endo-MEGs, and H3K4me3 and H3K36me3 methyltransferases could bind to endo-MEGs. *DME* is rarely expressed in sperm cells (Schoft et al., 2011), where the existence of CG hypermethylation around TSS inhibited the binding of transcriptional activators at endo-MEGs (Figure 5A). Hence, after fertilization, the endosperm inherits methylated paternal alleles and unmethylated maternal alleles with H3K4me3 and H3K36me3 modifications (Figure 5A).

Con-PEGs exhibited very similar expression levels in shoots and endosperms. Like all genes expressed in shoots, most con-PEGs (78.6%–88.6%) possessed H3K4me3 and H3K36me3 peaks but a very low proportion of H3K27me3 peaks (Supplemental Figure 11). DNA methylation was generally depleted in the 5′ ends of con-PEGs, and a high level of DNA methylation exists in the gene body of con-PEGs in shoots (Zhang et al., 2014a). In endosperm, con-PEGs were significantly associated with CG_pDMRs, pH3K4me3, pH3K36me3, and mH3K27me3 peaks, which indicates that the epigenetic profiles on active paternal alleles in endosperm agreed well with those in shoots. Most *Arabidopsis* con-PEGs (84.6%) did not express in central cells (Supplemental Table 5), and 67.7% of rice con-PEGs expressed in sperm cells (Supplemental Table 6). Therefore, we inferred that the monoallelic expression of con-PEGs is likely to be the silence of maternal alleles with the epigenetic switch involving the replacement from H3K4me3 and H3K36me3 modifications to H3K27me3 in central cells. But why was PRC2 complex recruited in central cells for these con-PEGs? We found that the gene body of con-PEGs exhibited maternal hypomethylation and paternal hypermethylation in endosperm. Recent studies showed that gene body methylation was positively correlated with H3K36me3 and negatively correlated with H3K27me3 (Ball et al., 2009; Kobayashi et al., 2012; Lou et al., 2014). So we hypothesize that DNA demethylation may occur in gene body regions for con-PEGs in central cells, which provides the opportunity for recruitment of PRC2 complex (Figure 5B). In sperm cells, a high level of methylation in the gene body inhibits the combination of PRC2 complex (Figure 5B). Hence, after fertilization, the endosperm inherits an active paternal allele with H3K4me3 and H3K36me3 modifications and repressed maternal alleles with H3K27me3 modifications (Figure 5B).

Endo-PEGs were silenced in shoots and possessed a low proportion (20%–35%) of H3K4me3 and H3K36me3 peaks but a high proportion of H3K27me3 peaks in shoots (Supplemental Figure 11). Similar epigenetic profiles were observed in silenced maternal alleles of endo-PEGs in endosperm (Figure 5C), indicating the imprinting expression of endo-PEGs is likely to be caused by erasing H3K27me3 and adding H3K4me3 and H3K36me3 modifications on paternal alleles. Furthermore, activation of paternal alleles of endo-PEGs seems to occur after fertilization as most rice endo-PEGs (83.3%) were not expressed in sperm cells (Supplemental Table 6). Recent evidence in *Arabidopsis* sperm cells showed that the H3.1 variant is completely absent while the H3.10 variant specifically accumulated on chromatin, which may be a specific histone variant immune for H3K27me3 because male generative nuclei were strongly reduced in H3K27me3 compared with vegetative nuclei in plants (Johnson et al., 2004; Sano and Tanaka, 2010; Houben et al., 2011; Borg and Berger, 2015). After fertilization, the paternally inherited H3.10 is removed from the zygote and early endosperm, and the H3.1 and H3.3 variants again occupy most of the paternal chromatin (Ingouff et al., 2007, 2010). Thus, we speculated that loading of H3.10 possibly contributes to the loss of H3K27me3 modifications in maize sperm cells. After fertilization, the imprinting expression of endo-PEGs is likely

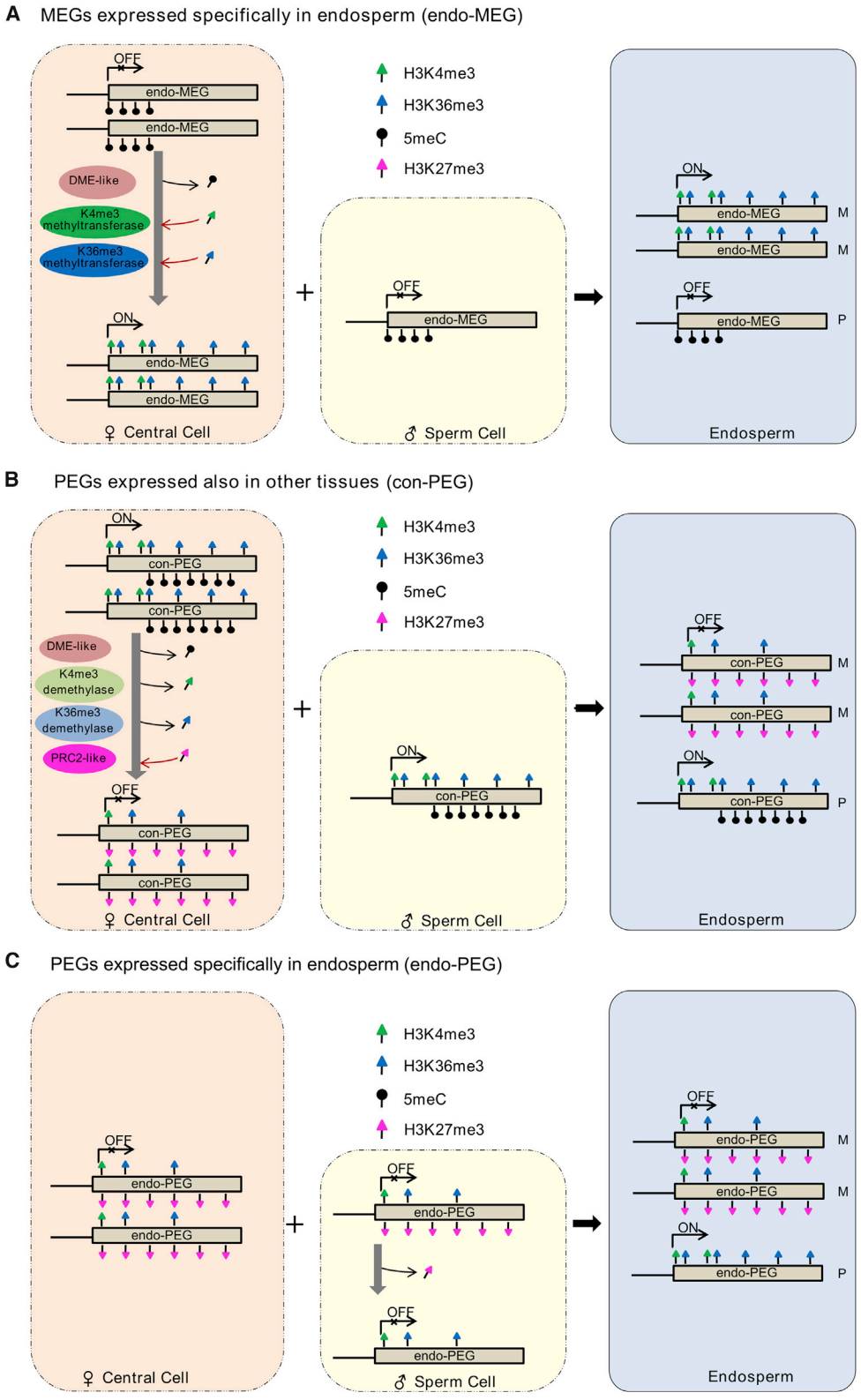

Figure 5. Possible Model of Epigenetic Silencing and Activating Dynamics at Imprinted Genes.

(A) Model for MEGs specifically expressed in endosperm (endo-MEG). In somatic tissues, hypermethylation around TSS inhibited the expression of both maternal allele and paternal allele. In central cells, the methylation around TSS can be removed by DME-like demethylase facilitating the combination of H3K4me3 and H3K36me3 methyltransferases, but not in sperm cells. After fertilization, DMRs exhibiting maternal demethylation and paternal hypermethylation, and maternally preferred H3K4me3 and H3K36me3 peaks were identified in the endosperm.

(legend continued on next page)

due to the failure of H3K27me3 deposition and the combination of H3K4me3 and H3K36me3 modifications on paternal alleles of endo-PEGs. Whether selective retention of the H3.10 variant on paternal alleles of endo-PEGs or other reasons after fertilization contribute to the failure of H3K27me3 deposition remains to be explored.

MNCs May Have Potentially Specified Roles in Endosperm

In mammals, the deletion of imprinting control regions results in the loss of the imprinted non-coding RNAs, which coincides with the loss of imprinting of protein-coding genes in the locus (Chamberlain and Brannan, 2001). However, studies on the mechanisms of epigenetic regulation of imprinted non-coding RNAs are very limited in plants. In our study, the profile of epigenetic modifications at MNCs accorded well with that of endo-MEGs, which associate with pDMRs, mH3K4me3, and mH3K36me3 peaks. Hence, the monoallelic expression of MNCs may have a very similar regulatory mechanism to that of endo-MEGs we proposed above.

In this study, we identified 35 MNCs and just a few PNCs in 12 DAP maize endosperm. Likewise, 40% of mH3K4me3 and mH3K36me3 peaks were located in intergenic/intronic regions, while about 90% of pH3K4me3 and pH3K36me3 peaks were located around genes, again suggesting that MNCs (marked by the mH3K4me3 and mH3K36me3 peaks in intergenic/intronic regions) may far outnumber PNCs in maize endosperm. Very similarly in rice, the number of candidate MNCs is about six times than that of candidate PNCs (Luo et al., 2011). Therefore, MNCs may have potentially specific roles in endosperm. Antisense lncRNAs could regulate epigenetic silencing, transcription, and mRNA stability of their adjacent genes (Carrieri et al., 2012). COOLAIR may possibly be an example mediating the coordinated switching of chromatin states at FLC during vernalization (Csorba et al., 2014). Hence, antisense MNCs probably regulate expression of their adjacent PEGs. One MNC located in the promoter of *ZmYucc1* (endo-PEG), where the weight of mutant in kernel (dry mass) was reported to be approximately 40% less than that of wild-type (Bernardi et al., 2012). The results would be very valuable to further explore the roles of imprinted long non-coding RNAs in maize.

METHODS

Tissue Collection

The maize (*Zea mays*) inbred lines B73 and Mo17 were grown in the field in Beijing. Three ears of reciprocal crosses of B73 and Mo17 were collected 12 and 14 DAP. Endosperm tissues were collected from three different ears by manual dissection from whole kernels and were immediately frozen in liquid nitrogen.

Library Construction for RNA-Seq and ChIP-Seq

RNA-seq was performed according to the protocol described in our previous work (Zhang et al., 2011), using 12 DAP endosperm of the reciprocal crosses of B73 and Mo17 collected above.

Strand-specific RNA-seq was performed using the 14 DAP endosperm of reciprocal crosses of B73 and Mo17. Total RNA was extracted from the nuclei. The RNA-seq libraries were constructed using TruSeq Stranded Total RNA with Ribo-Zero Plant kits (Illumina, catalog no. RS-122-2401) according to the manufacturer's instructions. Then, the quality and quantity of these libraries were analyzed by using the BioAnalyzer 2100 system and qPCR.

The ChIP assay of 12 DAP endosperm of reciprocal crosses of B73 and Mo17 was performed according to the protocol described in a previous study (Liu et al., 2008). The libraries for ChIP-seq followed the standard construction protocol.

Identification and Expression Analysis of Imprinted Genes and Imprinted Non-coding RNAs

The RNA-seq reads were mapped using the TopHat software (Trapnell et al., 2012). Then, the imprinted genes were identified with the same strategy used in previous works (Zhang et al., 2011, 2014a). Candidate imprinted protein-coding genes and non-coding RNAs were analyzed manually (Zhang et al., 2011). The strand of imprinted non-coding RNAs was according to the information from the strand-specific RNA-seq data. The strand of MNCs can be ensured if more than 20 strand-specific reads mapped on MNCs and >95% of them are from one strand.

Identification of Allele-Specific H3K4me3 and H3K36me3 Peaks

ChIP-seq reads were mapped to the B73 reference genome using Bowtie (Langmead et al., 2009). The endosperm H3K4me3 and H3K36me3 peaks were identified using MACS (Feng et al., 2012) with similar parameters used in our previous work (Zhang et al., 2014a). Peaks with at least two SNPs and with at least 10 reads on both B73 and Mo17 alleles were used for allele-specific peak analysis. Final maternally preferred H3K4me3 or H3K36me3 peaks were identified for those with at least 85% of reads derived from maternal alleles in both reciprocal hybrids. Paternally preferred H3K4me3 or H3K36me3 peaks were identified for those with at least 60% of reads derived from paternal alleles in both reciprocal hybrids.

ACCESSION NUMBERS

Data generated in this study are deposited in NCBI Sequence Read Archive under accession number SRP074869.

SUPPLEMENTAL INFORMATION

Supplemental Information is available at *Molecular Plant Online*.

FUNDING

This research was supported by the National Natural Science Foundation of China (31225020; 91435206; 31421005), and the 948 project (2016-X33).

(B) Model for PEGs expressed in many tissues (con-PEG). In somatic tissues, both the maternal allele and paternal allele were deposited with H3K4me3 around TSS and H3K36me3 in the gene body. In central cells, demethylation in the gene body facilitates the combination of PRC2 complex, which may recruit H3K4me3 and H3K36me3 demethylase to erase H3K4me3 and H3K36me3. But in sperm cells, hypermethylation in the gene body and the H3K4me3 around TSS and H3K36me3 persists. In the endosperm, H3K27me3 only targeted the demethylated maternal alleles, while H3K4me3 and H3K36me3 prefer to enrich on paternal alleles with hypermethylated gene body.
(C) Model for PEGs specifically expressed in endosperm (endo-PEG). In somatic tissues, H3K27me3 modifications were deposited on the whole body of endo-PEGs. H3.10-like variant specifically accumulating on sperm cells leads to loss of H3K27me3. After fertilization, H3K4me3 and H3K36me3 modifications preferred to deposit on paternal chromosomes without H3K27me3 modifications.
The dashed boxes around the central cells and sperm cells indicate that we do not have enough data to support the epigenetic status on imprinted genes.

AUTHOR CONTRIBUTIONS

X.D., J.C., and J.L. designed the experiments. X.D and J.C. collected all the materials. M.Z. and J.C preformed ChIP-seq and RNA-seq. X.D. performed bioinformatics analyses of all data. X.D. and J.L. wrote the manuscript. All authors read and approved the final manuscript.

ACKNOWLEDGMENTS

M.Z. was a postdoctoral fellow at Stanford University during the data analysis and manuscript writing and editing and was supported by the International Postdoctoral Exchange Fellowship Program (no. 20140067). We thank all projects for generating and sharing the data used in this paper. No conflict of interest declared.

Received: July 6, 2016
Revised: October 10, 2016
Accepted: October 10, 2016
Published: October 24, 2016

REFERENCES

Anderson, S.N., Johnson, C.S., Jones, D.S., Conrad, L.J., Gou, X., Russell, S.D., and Sundaresan, V. (2013). Transcriptomes of isolated *Oryza sativa* gametes characterized by deep sequencing: evidence for distinct sex-dependent chromatin and epigenetic states before fertilization. Plant J. **76**:729–741.

Ball, M.P., Li, J.B., Gao, Y., Lee, J.H., LeProust, E.M., Park, I.H., Xie, B., Daley, G.Q., and Church, G.M. (2009). Targeted and genome-scale strategies reveal gene-body methylation signatures in human cells. Nat. Biotechnol. **27**:361–368.

Barski, A., Cuddapah, S., Cui, K., Roh, T.Y., Schones, D.E., Wang, Z., Wei, G., Chepelev, I., and Zhao, K. (2007). High-resolution profiling of histone methylations in the human genome. Cell **129**:823–837.

Bernardi, J., Lanubile, A., Li, Q.B., Kumar, D., Kladnik, A., Cook, S.D., Ross, J.J., Marocco, A., and Chourey, P.S. (2012). Impaired auxin biosynthesis in the defective endosperm18 mutant is due to mutational loss of expression in the ZmYuc1 gene encoding endosperm-specific YUCCA1 protein in maize. Plant Physiol. **160**:1318–1328.

Borg, M., and Berger, F. (2015). Chromatin remodelling during male gametophyte development. Plant J. **83**:177–188.

Brien, G.L., Gambero, G., O'Connell, D.J., Jerman, E., Turner, S.A., Egan, C.M., Dunne, E.J., Jurgens, M.C., Wynne, K., Piao, L., et al. (2012). Polycomb PHF19 binds H3K36me3 and recruits PRC2 and demethylase NO66 to embryonic stem cell genes during differentiation. Nat. Struct. Mol. Biol. **19**:1273–1281.

Cabili, M.N., Trapnell, C., Goff, L., Koziol, M., Tazon-Vega, B., Regev, A., and Rinn, J.L. (2011). Integrative annotation of human large intergenic noncoding RNAs reveals global properties and specific subclasses. Genes Dev. **25**:1915–1927.

Carrieri, C., Cimatti, L., Biagioli, M., Beugnet, A., Zucchelli, S., Fedele, S., Pesce, E., Ferrer, I., Collavin, L., Santoro, C., et al. (2012). Long non-coding antisense RNA controls Uchl1 translation through an embedded SINEB2 repeat. Nature **491**:454–457.

Chamberlain, S.J., and Brannan, C.I. (2001). The Prader-Willi syndrome imprinting center activates the paternally expressed murine Ube3a antisense transcript but represses paternal Ube3a. Genomics **73**:316–322.

Csorba, T., Questa, J.I., Sun, Q., and Dean, C. (2014). Antisense COOLAIR mediates the coordinated switching of chromatin states at FLC during vernalization. Proc. Natl. Acad. Sci. USA **111**:16160–16165.

Du, M., Luo, M., Zhang, R., Finnegan, E.J., and Koltunow, A.M. (2014). Imprinting in rice: the role of DNA and histone methylation in modulating parent-of-origin specific expression and determining transcript start sites. Plant J. **79**:232–242.

Feng, J., Liu, T., Qin, B., Zhang, Y., and Liu, X.S. (2012). Identifying ChIP-seq enrichment using MACS. Nat. Protoc. **7**:1728–1740.

Gehring, M., Missirian, V., and Henikoff, S. (2011). Genomic analysis of parent-of-origin allelic expression in *Arabidopsis thaliana* seeds. PLoS One **6**:e23687.

Guenther, M.G., Levine, S.S., Boyer, L.A., Jaenisch, R., and Young, R.A. (2007). A chromatin landmark and transcription initiation at most promoters in human cells. Cell **130**:77–88.

Gutierrez-Marcos, J.F., Costa, L.M., Biderre-Petit, C., Khbaya, B., O'Sullivan, D.M., Wormald, M., Perez, P., and Dickinson, H.G. (2004). Maternally expressed gene1 Is a novel maize endosperm transfer cell-specific gene with a maternal parent-of-origin pattern of expression. Plant Cell **16**:1288–1301.

Gutierrez-Marcos, J.F., Costa, L.M., Dal Pra, M., Scholten, S., Kranz, E., Perez, P., and Dickinson, H.G. (2006). Epigenetic asymmetry of imprinted genes in plant gametes. Nat. Genet. **38**:876–878.

Haun, W.J., and Springer, N.M. (2008). Maternal and paternal alleles exhibit differential histone methylation and acetylation at maize imprinted genes. Plant J. **56**:903–912.

Haun, W.J., Laoueille-Duprat, S., O'Connell, M.J., Spillane, C., Grossniklaus, U., Phillips, A.R., Kaeppler, S.M., and Springer, N.M. (2007). Genomic imprinting, methylation and molecular evolution of maize Enhancer of zeste (Mez) homologs. Plant J. **49**:325–337.

He, G., Chen, B., Wang, X., Li, X., Li, J., He, H., Yang, M., Lu, L., Qi, Y., Wang, X., et al. (2013). Conservation and divergence of transcriptomic and epigenomic variation in maize hybrids. Genome Biol. **14**:R57.

Houben, A., Kumke, K., Nagaki, K., and Hause, G. (2011). CENH3 distribution and differential chromatin modifications during pollen development in rye (*Secale cereale* L.). Chromosome Res. **19**:471–480.

Hsieh, T.F., Shin, J., Uzawa, R., Silva, P., Cohen, S., Bauer, M.J., Hashimoto, M., Kirkbride, R.C., Harada, J.J., Zilberman, D., et al. (2011). Regulation of imprinted gene expression in *Arabidopsis* endosperm. Proc. Natl. Acad. Sci. USA **108**:1755–1762.

Huh, J.H., Bauer, M.J., Hsieh, T.F., and Fischer, R.L. (2008). Cellular programming of plant gene imprinting. Cell **132**:735–744.

Ibarra, C.A., Feng, X., Schoft, V.K., Hsieh, T.F., Uzawa, R., Rodrigues, J.A., Zemach, A., Chumak, N., Machlicova, A., Nishimura, T., et al. (2012). Active DNA demethylation in plant companion cells reinforces transposon methylation in gametes. Science **337**:1360–1364.

Ingouff, M., Hamamura, Y., Gourgues, M., Higashiyama, T., and Berger, F. (2007). Distinct dynamics of HISTONE3 variants between the two fertilization products in plants. Curr. Biol. **17**:1032–1037.

Ingouff, M., Rademacher, S., Holec, S., Soljic, L., Xin, N., Readshaw, A., Foo, S.H., Lahouze, B., Sprunck, S., and Berger, F. (2010). Zygotic resetting of the HISTONE 3 variant repertoire participates in epigenetic reprogramming in *Arabidopsis*. Curr. Biol. **20**:2137–2143.

Jahnke, S., and Scholten, S. (2009). Epigenetic resetting of a gene imprinted in plant embryos. Curr. Biol. **19**:1677–1681.

Johnson, L., Mollah, S., Garcia, B.A., Muratore, T.L., Shabanowitz, J., Hunt, D.F., and Jacobsen, S.E. (2004). Mass spectrometry analysis of *Arabidopsis* histone H3 reveals distinct combinations of post-translational modifications. Nucleic Acids Res. **32**:6511–6518.

Jullien, P.E., Kinoshita, T., Ohad, N., and Berger, F. (2006). Maintenance of DNA methylation during the *Arabidopsis* life cycle is essential for parental imprinting. Plant Cell **18**:1360–1372.

Kawashima, T., and Berger, F. (2014). Epigenetic reprogramming in plant sexual reproduction. Nat. Rev. Genet. **15**:613–624.

Kermicle, J.L., and Alleman, M. (1990). Gametic imprinting in maize in relation to the angiosperm life cycle. Dev. Suppl., 9–14.

Kinoshita, T., Miura, A., Choi, Y., Kinoshita, Y., Cao, X., Jacobsen, S.E., Fischer, R.L., and Kakutani, T. (2004). One-way control of

FWA imprinting in *Arabidopsis* endosperm by DNA methylation. Science **303**:521–523.

Kobayashi, H., Sakurai, T., Imai, M., Takahashi, N., Fukuda, A., Yayoi, O., Sato, S., Nakabayashi, K., Hata, K., Sotomaru, Y., et al. (2012). Contribution of intragenic DNA methylation in mouse gametic DNA methylomes to establish oocyte-specific heritable marks. PLoS Genet. **8**:e1002440.

Kohler, C., Page, D.R., Gagliardini, V., and Grossniklaus, U. (2005). The *Arabidopsis thaliana* MEDEA Polycomb group protein controls expression of PHERES1 by parental imprinting. Nat. Genet. **37**:28–30.

Langmead, B., Trapnell, C., Pop, M., and Salzberg, S.L. (2009). Ultrafast and memory-efficient alignment of short DNA sequences to the human genome. Genome Biol. **10**:R25.

Li, X., Wang, X., He, K., Ma, Y., Su, N., He, H., Stolc, V., Tongprasit, W., Jin, W., Jiang, J., et al. (2008). High-resolution mapping of epigenetic modifications of the rice genome uncovers interplay between DNA methylation, histone methylation, and gene expression. Plant Cell **20**:259–276.

Li, L., Eichten, S.R., Shimizu, R., Petsch, K., Yeh, C.T., Wu, W., Chettoor, A.M., Givan, S.A., Cole, R.A., Fowler, J.E., et al. (2014). Genome-wide discovery and characterization of maize long non-coding RNAs. Genome Biol. **15**:R40.

Li, Q., Gent, J.I., Zynda, G., Song, J., Makarevitch, I., Hirsch, C.D., Hirsch, C.N., Dawe, R.K., Madzima, T.F., McGinnis, K.M., et al. (2015). RNA-directed DNA methylation enforces boundaries between heterochromatin and euchromatin in the maize genome. Proc. Natl. Acad. Sci. USA **112**:14728–14733.

Liu, Z., Yue, W., Li, D., Wang, R.R., Kong, X., Lu, K., Wang, G., Dong, Y., Jin, W., and Zhang, X. (2008). Structure and dynamics of retrotransposons at wheat centromeres and pericentromeres. Chromosoma **117**:445–456.

Lou, S., Lee, H.M., Qin, H., Li, J.W., Gao, Z., Liu, X., Chan, L.L., Kl, L.V., So, W.Y., Wang, Y., et al. (2014). Whole-genome bisulfite sequencing of multiple individuals reveals complementary roles of promoter and gene body methylation in transcriptional regulation. Genome Biol. **15**:408.

Lund, G., Ciceri, P., and Viotti, A. (1995a). Maternal-specific demethylation and expression of specific alleles of zein genes in the endosperm of *Zea mays* L. Plant J. **8**:571–581.

Lund, G., Messing, J., and Viotti, A. (1995b). Endosperm-specific demethylation and activation of specific alleles of alpha-tubulin genes of *Zea mays* L. Mol. Gen. Genet. **246**:716–722.

Luo, M., Taylor, J.M., Spriggs, A., Zhang, H., Wu, X., Russell, S., Singh, M., and Koltunow, A. (2011). A genome-wide survey of imprinted genes in rice seeds reveals imprinting primarily occurs in the endosperm. PLoS Genet. **7**:e1002125.

Pasini, D., Hansen, K.H., Christensen, J., Agger, K., Cloos, P.A., and Helin, K. (2008). Coordinated regulation of transcriptional repression by the RBP2 H3K4 demethylase and Polycomb-Repressive Complex 2. Genes Dev. **22**:1345–1355.

Raissig, M.T., Baroux, C., and Grossniklaus, U. (2011). Regulation and flexibility of genomic imprinting during seed development. Plant Cell **23**:16–26.

Rodrigues, J.A., Ruan, R., Nishimura, T., Sharma, M.K., Sharma, R., Ronald, P.C., Fischer, R.L., and Zilberman, D. (2013). Imprinted expression of genes and small RNA is associated with localized hypomethylation of the maternal genome in rice endosperm. Proc. Natl. Acad. Sci. USA **110**:7934–7939.

Sano, Y., and Tanaka, I. (2010). Distinct localization of histone H3 methylation in the vegetative nucleus of lily pollen. Cell Biol. Int. **34**:253–259.

Schmid, M.W., Schmidt, A., Klostermeier, U.C., Barann, M., Rosenstiel, P., and Grossniklaus, U. (2012). A powerful method for transcriptional profiling of specific cell types in eukaryotes: laser-assisted microdissection and RNA sequencing. PLoS One **7**:e29685.

Schmitges, F.W., Prusty, A.B., Faty, M., Stutzer, A., Lingaraju, G.M., Aiwazian, J., Sack, R., Hess, D., Li, L., Zhou, S., et al. (2011). Histone methylation by PRC2 is inhibited by active chromatin marks. Mol. Cell **42**:330–341.

Schoft, V.K., Chumak, N., Choi, Y., Hannon, M., Garcia-Aguilar, M., Machlicova, A., Slusarz, L., Mosiolek, M., Park, J.S., Park, G.T., et al. (2011). Function of the DEMETER DNA glycosylase in the *Arabidopsis thaliana* male gametophyte. Proc. Natl. Acad. Sci. USA **108**:8042–8047.

Tiwari, S., Schulz, R., Ikeda, Y., Dytham, L., Bravo, J., Mathers, L., Spielman, M., Guzman, P., Oakey, R.J., Kinoshita, T., et al. (2008). MATERNALLY EXPRESSED PAB C-TERMINAL, a novel imprinted gene in *Arabidopsis*, encodes the conserved C-terminal domain of polyadenylate binding proteins. Plant Cell **20**:2387–2398.

Trapnell, C., Roberts, A., Goff, L., Pertea, G., Kim, D., Kelley, D.R., Pimentel, H., Salzberg, S.L., Rinn, J.L., and Pachter, L. (2012). Differential gene and transcript expression analysis of RNA-seq experiments with TopHat and Cufflinks. Nat. Protoc. **7**:562–578.

Wang, X., Elling, A.A., Li, X., Li, N., Peng, Z., He, G., Sun, H., Qi, Y., Liu, X.S., and Deng, X.W. (2009). Genome-wide and organ-specific landscapes of epigenetic modifications and their relationships to mRNA and small RNA transcriptomes in maize. Plant Cell **21**:1053–1069.

Waters, A.J., Makarevitch, I., Eichten, S.R., Swanson-Wagner, R.A., Yeh, C.T., Xu, W., Schnable, P.S., Vaughn, M.W., Gehring, M., and Springer, N.M. (2011). Parent-of-origin effects on gene expression and DNA methylation in the maize endosperm. Plant Cell **23**:4221–4233.

Waters, A.J., Bilinski, P., Eichten, S.R., Vaughn, M.W., Ross-Ibarra, J., Gehring, M., and Springer, N.M. (2013). Comprehensive analysis of imprinted genes in maize reveals allelic variation for imprinting and limited conservation with other species. Proc. Natl. Acad. Sci. USA **110**:19639–19644.

Widiez, T., Symeonidi, A., Luo, C., Lam, E., Lawton, M., and Rensing, S.A. (2014). The chromatin landscape of the moss *Physcomitrella patens* and its dynamics during development and drought stress. Plant J. **79**:67–81.

Wolff, P., Weinhofer, I., Seguin, J., Roszak, P., Beisel, C., Donoghue, M.T., Spillane, C., Nordborg, M., Rehmsmeier, M., and Kohler, C. (2011). High-resolution analysis of parent-of-origin allelic expression in the *Arabidopsis* Endosperm. PLoS Genet. **7**:e1002126.

Wu, Y., Kikuchi, S., Yan, H., Zhang, W., Rosenbaum, H., Iniguez, A.L., and Jiang, J. (2011). Euchromatic subdomains in rice centromeres are associated with genes and transcription. Plant Cell **23**:4054–4064.

Xin, M., Yang, R., Li, G., Chen, H., Laurie, J., Ma, C., Wang, D., Yao, Y., Larkins, B.A., Sun, Q., et al. (2013). Dynamic expression of imprinted genes associates with maternally controlled nutrient allocation during maize endosperm development. Plant Cell **25**:3212–3227.

Yang, H., Howard, M., and Dean, C. (2014). Antagonistic roles for H3K36me3 and H3K27me3 in the cold-induced epigenetic switch at *Arabidopsis* FLC. Curr. Biol. **24**:1793–1797.

Zhan, J., Thakare, D., Ma, C., Lloyd, A., Nixon, N.M., Arakaki, A.M., Burnett, W.J., Logan, K.O., Wang, D., Wang, X., et al. (2015). RNA sequencing of laser-capture microdissected compartments of the maize kernel identifies regulatory modules associated with endosperm cell differentiation. Plant Cell **27**:513–531.

Zhang, X., Bernatavichute, Y.V., Cokus, S., Pellegrini, M., and Jacobsen, S.E. (2009). Genome-wide analysis of mono-, di- and

trimethylation of histone H3 lysine 4 in *Arabidopsis thaliana*. Genome Biol. **10**:R62.

Zhang, M., Zhao, H., Xie, S., Chen, J., Xu, Y., Wang, K., Zhao, H., Guan, H., Hu, X., Jiao, Y., et al. (2011). Extensive, clustered parental imprinting of protein-coding and noncoding RNAs in developing maize endosperm. Proc. Natl. Acad. Sci. USA **108**:20042–20047.

Zhang, M., Xie, S., Dong, X., Zhao, X., Zeng, B., Chen, J., Li, H., Yang, W., Zhao, H., Wang, G., et al. (2014a). Genome-wide high resolution parental-specific DNA and histone methylation maps uncover patterns of imprinting regulation in maize. Genome Res. **24**:167–176.

Zhang, Y.C., Liao, J.Y., Li, Z.Y., Yu, Y., Zhang, J.P., Li, Q.F., Qu, L.H., Shu, W.S., and Chen, Y.Q. (2014b). Genome-wide screening and functional analysis identify a large number of long noncoding RNAs involved in the sexual reproduction of rice. Genome Biol. **15**:512.

Zhang, M., Li, N., He, W., Zhang, H., Yang, W., and Liu, B. (2016). Genome-wide screen of genes imprinted in sorghum endosperm, and the roles of allelic differential cytosine methylation. Plant J. **85**:424–436.